(4)

REPORT DOCUMENTATION PAGE

Form Approved
OMB No. 0704-0188

1. AGENCY USE ONLY (Leave blank)	2. REPORT DATE	3. REPORT TYPE AND DATES COVERED
	6/29/90	Final Report

4. TITLE AND SUBTITLE
Polycrystalline Diamond Junction Field Effect Transistors (JFETS)1

5. FUNDING NUMBERS
C N00014-89-C-0150
PE 63220
P S405018
TA 8rr
WU 01

6. AUTHOR(S)
Maurice Landstrass and Dale Moyer

7. PERFORMING ORGANIZATION NAME(S) AND ADDRESS(ES)
Crystallume
125 Constitutution Drive
Menlo Park, CA 94025

8. PERFORMING ORGANIZATION REPORT NUMBER

9. SPONSORING/MONITORING AGENCY NAME(S) AND ADDRESS(ES)
SDIO/IST
ONR, Code 1114
Arlington, VA 22217

10. SPONSORING/MONITORING AGENCY REPORT NUMBER
N/A

AD-A223 784

11. SUPPLEMENTARY NOTES

12a. DISTRIBUTION/AVAILABILITY STATEMENT
Approved for public release; distributuion unlimited

12b. DISTRIBUTION CODE
N/A

13. ABSTRACT
Diodes were fabricated from in situ doped "N"-diamond/P-diamond layer structures. The "N"-dopants investigated were nitrogen and oxygen. All diode stuctures were fabricated on insulating diamond substrates. The properties of diodes fabricated from boron doped diamond films was investigated in the resistivity range from 2.0 Ohm-cm to 2.7 x 10^{-3} Ohm-cm. All aluminum Schottky diodes fabricated in this range were completely Ohmic showing no evidence of rectification. Junction diodes using nitrogen or oxygen doped layers were fabricated that had signifcant rectification. Diodes fabricated using this design had a serious dificulty with excessive series resistance. As these diodes are designed to be gate electrodes, series resistance may be acceptable. The diode n-diamond doping levels are limited by the currently achievable donor dopant concentrations to approximately 1.0 x 10^{19} cm^{-3}. Electron channelling measurements were performed on epitaxial diamond layers grown on type IIA natural diamond. These measurements confirmed the epitaxial relationship between CVD diamond layers grown in the plasma apparatus used for this study. All doped layers processes used in this study were developed so as to grow single crystal diamond on single crystal diamond substrates.

14. SUBJECT TERMS	15. NUMBER OF PAGES
Diamond, Transistors, JFET, Doping, Epitaxy	36
	16. PRICE CODE

17. SECURITY CLASSIFICATION OF REPORT	18. SECURITY CLASSIFICATION OF THIS PAGE	19. SECURITY CLASSIFICATION OF ABSTRACT	20. LIMITATION OF ABSTRACT
UNCLAS	UNCLAS	UNCLAS	SAR

NSN 7540-01-280-5500

Standard Form 298 (Rev. 2-89)
Prescribed by ANSI Std. Z39-18
298-102

SDIO/N00014-89-C-0150

POLYCRYSTALLINE DIAMOND JUNCTION FIELD EFFECT TRANSISTORS (JFETs)

FINAL REPORT

Maurice I. Landstrass and Dale Moyer

CRYSTALLUME
125 Constitution Drive
Menlo Park, CA 94025

June 30, 1990

[1]*Research supported by SDIO/IST and managed by the Office of Naval Research*

POLYCRYSTALLINE DIAMOND JUNCTION FIELD EFFECT TRANSISTORS (JFETS)[1]

Final Report
June 30, 1990
Maurice Landstrass, Dale Moyer

Results Summary

Diodes were fabricated from in situ doped "N"-diamond/P-diamond layer structures. The "N"-dopants investigated were nitrogen and oxygen. All diode structures were fabricated on insulating diamond substrates. The properties of diodes fabricated from boron doped diamond films was investigated in the resistivity range from 2.0 Ohm-cm to 2.7 x 10^{-3} Ohm-cm. All aluminum Schottky diodes fabricated in this range were completely Ohmic showing no evidence of rectification. Junction diodes using nitrogen or oxygen doped layers were fabricated that had significant rectification. Diodes fabricated using this design had a serious difficulty with excessive series resistance. As these diodes are designed to be gate electrodes, series resistance may be acceptable. SIMS measurements were performed on polycrystalline diamond films and diode structures to evaluate the doping efficiency of boron, nitrogen and oxygen. Boron doping efficiency was found to be very high with measured maximum doping concentrations (polydiamond) of 1.7 x 10^{21} boron per cm^{-3} based on an in-sample ion implanted boron calibration. The dopant concentrations, as measured by SIMS, of both nitrogen and oxygen was found to be too low, in the films analyzed, to create the ideal desired N+(deep donor)/P+(boron) diamond diodes. The diode n-diamond doping levels are limited by the currently achievable donor dopant concentrations to approximately 1.0 x 10^{19} cm^{-3}. Electron channelling measurements were performed on epitaxial diamond layers grown on type IIA natural diamond. These measurements confirmed the epitaxial relationship between CVD diamond layers grown in the plasma apparatus used for this study. All doped layers processes used in this study were developed so as to grow single crystal diamond on single crystal diamond substrates.

Introduction

Diamond's large band gap and high carrier mobility has special attraction for use as a semiconductor material. Diamond based semiconductor devices should be able to operate at high temperatures and at high frequencies and should, in principle, be superior to devices fabricated in other semiconductors. In addition the wide band gap should also make diamond insulators and passivation significantly more immune to the effects of ionizing radiation as compared to other common device isolation such as silicon dioxide (SiO_2).

Diamond transistors have the potential of being the ideal device for operation in extreme environments. One of the most important properties of diamond is its exceptional thermal conductivity. Heat developed in a transistor is highly localized to small sections of the device such as near the drain region of a FET. The main factor in determining the device temperature is heat spreading through the semiconductor substrate. Since waste heat production is proportional to the device temperature, a diamond device would be able to operate at much higher power levels than a silicon device operating at the same temperature if both devices have the same gain. Under conditions of constant power output the temperature of the device is controlled by a positive or runaway type feedback due to the resistance decreasing with temperature. The device thermal conductivity determines the gain and response time in this thermal circuit. In a complex integrated circuit the instantaneous power output can vary from uniform distribution across a circuit to local heating due to an adjacent device or due to a large signal input to a single device. All these heat sources can be controlled if a large thermal conductivity material such as diamond is used to fabricate the circuits.

The ability to synthesize diamond films at temperatures and pressures more in keeping with widely adaptable industrial practices makes the prospects for diamond based semiconductor devices more tangible. However, an important requirement is single crystal diamond film for device fabrication. Another major requirement is the need for dopant and device design technology specific to the unique requirements of diamond.

The growth of single crystal diamond film requires that epitaxy be possible in the deposition process. This requires a process that grows diamond but does not nucleate diamond. The obvious first step is the growth of homoepitaxial diamond on natural or high pressure synthesized diamond single crystals. The other alternative is heteroepitaxy. Of the potential

substrates for heteroepitaxial growth of diamond, nickel and copper have the closest lattice match to diamond.

As a consequence of the difficulties involved in growing single crystal diamond films, opportunities for the use of polycrystalline diamond films in semiconductor electronics have to be explored. The growth of polycrystalline diamond films is a technology that is undergoing active development around the world. In the work reported here, the main focus of the development is the utilization of polycrystalline diamond films.

In order to assure wide application of the results single crystal diamond homoepitaxy was also performed using the same processes.

Diamond JFETs

The overall objective of this work is to develop a diamond junction field effect transistor (JFET) technology. Figure 1 is a schematic cross section of the proposed transistor configuration. One of the major reasons for choosing a JFET configuration is that it allows more flexibility in designing a diamond transistor. Table 1 lists some of the advantages of diamond with respect to *silicon and gallium arsenide*. A *diamond transistor design* that can take advantage of these properties has proved problematic[1,2,3]. A JFET design takes advantage of the beneficial properties of diamond without being penalized by some of problem areas. Specifically the high mobility, high velocity, large breakdown field and high bandgap are positive areas whereas the lack of shallow p dopants and any n dopants are problem areas. Another significant problem is the small built in diode voltage that has been achieved to date4. A major requirement is the need for dopant and device design technology specific to the unique requirements of diamond.

The JFET transistor design is an approach that takes advantage of diamonds large bandgap and utilizes this property to help overcome the lack of shallow dopants. The overall approach is to develop a diamond JFET technology through optimization of junction properties that can utilize near degenerate channel boron doping. The high doping levels are necessary to reduce the boron dopant activation energy. The primary approach is to control the built in junction voltage through nitrogen doping, control junction edge leakage with a passivation technology based on selective oxidation and heavily dope the channel with boron. Keywords: Diamond, Transistors, JFET, Doping, Epitaxy, Diodes, Fabrication, Nitrogen, Oxygen, Boron, Polycrystalline, Crystallography, Physics

Diamond Semiconductor Comparisons

Measurement	Si	GaAs	Natural Diamond (polycrystalline)
Band Gap *(eV)*	1.12	1.43	5.45
Hole Mobility *($cm^2/V\text{-}s$)*	480	400	1600
Electron Mobility *($cm^2/V\text{-}s$)*	1350	8800	1900
Breakdown Field *(V/cm)*	3.0×10^5	3.5×10^5	$1 \times 10^7 (3.5 \times 10^6)$
Electrical Resistivity (Max.) *(Ω-cm)*	1×10^3	1×10^9	1×10^{16}
Work Function *(eV)(P+)(approx.)*	5.2	5.1	5.5
Carrier Lifetime *(s)*	2.5×10^{-3}	10^{-8}	10^{-9}
Thermal Conductivity *(W/cm·K)*	1.45	0.46	20(18)
Electron Velocity *(cm/s)*	1×10^7	2×10^7	2.7×10^7
Dielectric Constant	11.7	13.1	5.5
Lattice Constant *(Å)*	5.43	5.65	3.57
Hardness *(kg/mm^2)*	1×10^3	6×10^2	1×10^4
Refractive Index	3.5	3.4	2.41
Thermal Expansion Coeff. *(K^{-1})*	2.6×10^{-6}	5.9×10^{-6}	0.8×10^{-6}
Melting Point *(°C)*	1420	1238	1527(decompose)

Table 1: Selected properties of diamond, silicon and gallium arsenide

Diamond Doping

Figure 2 is a band diagram of the proposed JFET gate structure structure. This device imposes several requirements on the different layers:

1. The channel doping has to be as high as possible,
2. The sheet doping of the gate has to be approximately the sheet doping of the channel,
3. The gate layer (nitrogen doped) has to be as thin as possible.

Boron Doping

The "heavy doping" requirement comes from the very high boron dopant activation energy of 0.4eV. The activation energy boron in diamond is a function of dopant concentration and can approach reasonable values (.05eV) only at high doping levels. In a JFET the gain is proportional to conductivity per dopant atom and it is the total dopant dopant concentration, independent of

ionization, that is important. As a result of this effect in diamond, impurity ionization energy reduction is a first order design consideration of a doped channel JFET.

Boron doping experiments were performed in a DC plasma reactor equipped with facilities to safely handle up to 1% diborane diluted in hydrogen. The main variables explored were substrate choice and type, temperature and diborane concentration. In order to investigate the junction properties of devices fabricated from these layers, the boron doped films were grown considerably thicker (~1.0 micron) than optimum for a JFET channel. These thick films are necessary to reduce the diode series resistance but would be unable to be fully depleted in a JFET configuration. All runs have employed diamond substrates. This approach mirrors the requirements for channel growth (except for controlled thickness) while avoiding the added complications associated with diamond nucleation.

The main emphasis has been to explore the in situ high concentration doping regime. Film growth has been performed using diborane concentration ranging to approximately 8000ppm diborane to methane concentration in the gas phase. The maximum concentration is not precisely known due to the observed plating of boron on various reactor parts during growth. All the films grown were conductive and all the films were determined to be diamond from their Raman spectra. The minimum resistivity obtained thus far has been 2.7×10^{-3} Ohm-cm. The incorporation ratio, which describes the boron incorporated into the diamond lattice as a function of the gas phase boron concentration, is approximately the value deduced from ref. 1. This agreement is very close considering the many differences between microwave and DC plasma diamond deposition. The boron concentration in the diamond lattice is higher than in the gas phase.

Figure 3 is a plot of the injected diborane to methane gas concentration ratio versus film resistivity. The resistivity plot in Fig. 3 exhibits a well behaved linear dependence on diborane concentration throughout the range plotted. This behavior suggests simple dopant incorporation on substitutional lattice sites without significant precipitation. Also in contrast to polysilicon behavior there is no resistance increase, due to grain boundaries, at the lower dopant concentrations. The high concentration films were investigated by two separate SIMS studies and found to contain $1.7 \times 10^{21} cm^{-3}$ boron. This concentration suggests possible massive precipitation of boron yet this conclusion is <u>not</u> supported by the data. Boron precipitates, as observed by SIMS, add significant noise to the measured profile which is not observed in the profile of Fig. 4 or Fig. 5. These profiles have a depth sensitivity of 5.0nm. The smooth profile puts an upper limit of 5.0nm on the size of any possible precipitates. The peak concentration value was calculated from Fig.5 using a boron ion implant placed into an undoped diamond layer grown on top of the boron doped film. This implant served as the SIMS calibration standard. Figure 5 is a recording of the profile of this

sample. The initial bump in the profile is the boron implant. The undoped layer allows a clear measurement of the implant.

Diamond has a very high atomic density of 1.75 x $10^{23}cm^{-3}$ when compared to 5.0 x $10^{22}cm^{-3}$ for silicon. SIMS is a precise technique with a long history in the analysis of silicon and gallium arsenide, but its use on diamond is new, especially so for CVD diamond films. Even when adjusted for the high atom density, the concentration of 1.0 atomic% boron in diamond is an exceptionally high value. While this value is comparable to the high temperature solid solubility of arsenic in silicon (4.0 atomic%) and that of boron in silicon (1.0 atomic%), low temperature CVD films typically do not achieve these high doping densities. The SIMS data appears to be in conflict with the well behaved dependence of film resistivity versus gas composition. Both the SIMS data and the resistivity are however in general agreement with published data[5,6].

A calculation of the doping density calibrated from the measured endpoint gives a doping range in Fig. 3 of $1.7x10^{21}cm^{-3}$ to $1.0x10^{18}cm^{-3}$. From other work[5,6] there is significant reduction in the boron activation energy in this dopant range. One of the key benefits in the JFET approach is that it provides a way to make a gate junction to a highly doped channel region. All devices have been fabricated from highly boron doped layers with an emphasis on dopant densities above $1.0x10^{20}cm^{-3}$.

Figure 6 plots the range of resistivities achieved using a solid boron doping source and similar growth conditions. This data implies that the observed doping in the present study is from the gas source and not the boron coated reactor components. This conclusion arises from the data showing that the minimum resistivity obtainable from the solid source is much higher (less doping) then from the present work (gas phase diborane).

A side effect of doping with boron is illustrated by the Raman spectra in Fig. 7. Boron doping, (in certain concentrations) eliminates the Raman signal from non diamond bonded carbon while either improving or simply not degrading the signal from the diamond bonds. The spectra in Fig. 7 were measured on material grown under similar DC plasma conditions using 0.3% methane in hydrogen. This has been reported before in the literature and is similar to the effect of oxygen on diamond growth[7]. This effect is quite pronounced on a DC plasma produced film due to the typically rich, detailed Raman spectra obtained from this material.

Nitrogen Doping

The second and third requirements for this device rely on controlled nitrogen doping of the gate layer. Nitrogen doping is not as straightforward to characterize as boron doping due to its electrical role as a deep donor. At normal temperatures deep donors are not ionized and do not create n-type conductive layers in proportion to the doping density. SIMS is the only technique that we have used that is readily able to determine the nitrogen doping density.

Figure 4 is a SIMS profile of a polydiamond pn junction doped with nitrogen and boron. The layers were grown to have the exact energy band structure as depicted in Fig. 2. The boron side was grown in a methane, hydrogen and diborane gas mixture with an 8000ppm boron to carbon concentration. The nitrogen doped side was grown in a methane, hydrogen and ammonia gas mixture with a 2.5% atomic nitrogen to carbon concentration. Both doped layers were grown on top of a 0.4 μm layer of undoped diamond. Figure 4 illustrates that the specific impurity incorporation varies strongly with dopant species when comparing boron to nitrogen.

From the data shown in Fig. 4, boron incorporates into the diamond lattice at a concentration proportionally higher than the gas phase concentration while nitrogen incorporates at substantially lower levels than the gas phase concentration. An interesting feature of these impurity profiles is the large concentration of nitrogen in the boron doped layer. The boron doped layer was grown in a gas ambient containing no intentionally added nitrogen. The boron doping reactor contained a 500 ppm nitrogen to carbon concentration in the gas phase as calculated from the specified feed gas impurity levels. The evidence suggest that the incorporation efficiency can be strongly dependent on the other dopants present in the diamond film.

The SIMS data in Fig. 4 clearly indicates that the structure fabricated does not meet the design requirements of a highly nitrogen doped diamond layer. The layer doping is far too low compared to the boron doped layer. As discussed above it is not desirable to decrease the boron doping so that device optimization demands a more efficient way to incorporate nitrogen. These results suggest that for CVD diamond films a co-dopant is necessary to achieve the high donor concentrations required for this device design.

Oxygen Doped Diamond

Oxygen is a double donor in silicon with unpredictable behavior. The electronic properties of oxygen dissolved in diamond are entirely unknown. Recently it has been reported that diamond films grown in an oxygen containing ambient behave functionally similar (as described above) to a diamond layer heavily doped with deep donors; i.e. permits a good junction to be made to material that otherwise would make leaky diodes[8]. Oxygen has an advantage over nitrogen as a dopant for CVD diamond in that films can be grown in oxygen ambients up to 50% by volume (flame growth). The compatibility allows for potentially higher dissolved oxygen concentration than with nitrogen. SIMS was performed on two samples grown in oxygen ambients, one in CO and one in O_2 with a 0.5 C/O ratio. The "dissolved" oxygen concentrations were $7.0x10^{17}cm^{-3}$ and $2.0x10^{18}cm^{-3}$. This data is summarized in table 2 . The word dissolved is in quotation marks due to the possibility that a large percentage of the oxygen is at the grain boundaries. The incorporation efficiency of oxygen using microwave growth is much lower than nitrogen using DC plasma growth. From this table and other data it appears that the solubility of both nitrogen and oxygen is much lower than that of boron.

sample	Boron(cm^{-3})	Oxygen(cm^{-3})	hydrogen(cm^{-3})	nitrogen(cm^{-3})
1(B)	1.7×10^{21}	1×10^{19}	3×10^{21}	7×10^{19}
2(B)	$1.7x\ 10^{21}$	5×10^{18}	$2.x\ 10^{21}$	1.2×10^{20}
2A(N)	3×10^{17}	3×10^{18}	3.5×10^{21}	3×10^{19}
3(CO)	3×10^{16}	7×10^{17}	5×10^{19}	3×10^{16}
4(O2)	7×10^{15}	2×10^{18}	3×10^{19}	3×10^{16}
5(un)	5×10^{16}	2×10^{18}	1×10^{20}	3×10^{16}
6(N)	5×10^{17}	1.5×10^{18}	2.5×10^{21}	1.5×10^{19}

Table 2: Selected SIMS data from 1. boron doped DC film, 2; boron doped DC film, nitrogen doped diode, 3; oxygen (CO) doped microwave film, 4; Oxygen doped microwave film(O2), 5; undoped microwave film, 6; nitrogen doped DC film

High Resistivity Substrates for Diamond Film Growth

The predominant structure used in this study is a pn junction, in situ doped, grown on a thick high resistivity diamond substrate. As in other "epitaxially grown" devices, the initial substrate determines many of the properties of the later epitaxial layers.

Two basic substrates are used in this work; high resistivity polycrystalline diamond grown in a "clean" reactor, and type IIA natural diamond with a (100) orientation.

The growth of large and small grained, polycrystalline diamond films has been performed in a separate reactor not plumbed with diborane in order to avoid boron cross contamination. The films grown thus far have had either a 0.2 micron nominal grain size or a 5 micron grain size. Most films in this work were grown using low pressure DC plasma diamond growth techniques. The sheet resistance of the films grown thus far exceeds our measurement capability due to "shorting" to the silicon substrate. The "effective sheet resistance" exceeds 1 x 10^{13} Ω/square and thus far has not presented any difficulty in characterizing the boron doped layers. The latter is due to the much lower sheet resistance (100-1000 Ωs/square) of the in situ boron doped diamond layers.

Type IIA, natural diamond, (100) substrates were purchased from Dubbledee-Harris. The dimensions of the samples were 1x1x0.1 mm. Prior to growth the substrates were ultrasonically cleaned in acetone (no other cleans have been employed). An array of nickel dots, 100 microns in diameter, were sputtered onto some of the samples.. These substrates, as received, had greater than 1 x 10^{14} Ω-cm resistivity which allowed for easy characterization of the boron doped grown layers.

Diamond Film Growth (General)

The desired device structure is composed of three layers; high resistivity diamond substrate, boron doped diamond active layer, and nitrogen doped diamond gate layer. Each of these layers impact the diode properties of the of the proposed JFET gate. Due to the very high doping efficiency of boron the three layers were grown in three separate reactors. This was necessary due to the high resistivity requirements of both the substrate and gate layer.

All boron doped layers were grown in a DC plasma reactor using mixtures of hydrogen, methane, and diborane gases. Nitrogen doped layers were also grown in a DC plasma reactor using mixtures of hydrogen, methane, and ammonia gases. Oxygen doped layers were grown in a microwave driven plasma reactor using mixtures of hydrogen, methane, and oxygen gases.

Electron channelling measurements were performed on diamond single crystals placed in the growth reactor during growth of the polycrystalline diamond films. Channelling measurements confirmed the epitaxial relationship of growth on these substrates.

Single Crystal Diamond Growth

Figure 8 is a Raman spectra recorded from a measurement performed on a boron doped single crystal layer grown at 725°C. In this figure the intensity scale is expanded, truncating the top of the diamond peak, so as to measure the signal from the epilayer. This spectra includes substantial signal from the natural diamond substrate. The Raman signal is virtually indistinguishable from the substrate. SEM (scanning electron microscope) micrographs of the growth surface show a definite morphology change indicative of growth. All the epilayer growths had electrical conductivity change due to the boron doped layer. The layer conductivity is independent of annealing in nitrogen which is indicative of boron doping rather than hydrogen passivation effects. All the boron doped films produced, both polycrystalline or single crystal, have had substantially lower resistivity (less than 0.1Ω-cm) than observed with undoped films in marked contrast to other other workers[7].

Boron doped, single crystal diamond layers behave differently from the polycrystalline layers grown to date. Cross-sectioned and stained samples have determined this to be due to large differences in growth rate when compared to the polydiamond samples. The major difference has been difficulty in growth rate control and/or nucleation control. There is little published literature on boron doped epitaxial diamond grown in a DC plasma reactor

Growth on the nickel dot region of the diamond substrate has also been quite different. From SEM examination, the surface morphology of the growth on the nickel dot is at least partly polycrystalline diamond. Figure 9 is a Raman spectra taken from the nickel dot region. Clearly distinguishable from the substrate, this area shows significant signal from non-diamond bonded carbon. In an electron beam induced voltage contrast enhanced image of the diamond substrate and epilayer, the nickel dot had markedly different contrast.. In this technique the sample is grounded from a single point and the SEM beam current induces a voltage drop across the sample In this sample the voltage drop occurs in the boron doped layer, on top of the insulating diamond substrate, and can be seen as a black "flame" emanating from the wire ground contact. Faintly discernable in the image is the array of nickel dots. More distinct is the voltage contrast of the nickel dot region. The contrast image of the nickel dot is a semi-circular bright contrast protrusion into the dark contrast "black flame" area This contrast indicates that in this region current is not flowing and sharply differentiates the nickel dot from the boron doped epilayer where the current is flowing to ground. This suggests the film grown in this region is not conductive. This contrast

can also be due to the nickel causing enhanced current recombination. These electrical properties of diamond grown in the vicinity of metallic nickel are suggestive of unforeseen problems associated with heteroepitaxial growth of diamond on nickel. At present it is unclear how the observed behavior interacts with the growth variables.

Figures 10 and 11 are backscattered electron channelling patterns recorded on both the substrate (Fig. 10) and the boron doped epilayer (Fig. 11). In this scanning electron microscope technique a collimated electron beam is impinged on the sample instead of the usual focused electron beam. The beam is tilted and the backscattered electron intensity is recorded as a function of angle. In these measurements the beam size was approximately 100 microns in diameter. The contrast mechanism in this technique is due to enhanced penetration of the e-beam into the solid when the beam impinges the sample at definite crystallographic angles. These patterns were produced using a beam energy of 5KeV which samples the first 0.5 microns in depth.

The clear channelling patterns obtained indicate both samples are single crystal. The major difference between the obtained patterns is the distortion apparent in the recording of Fig. 10. The substrate is a high resistivity type IIA diamond which develops a charge in the electron beam distorting the image. This also occurs in normal SEM imaging. The boron doped epilayer in Fig. 11 is conductive allowing for clear undistorted channelling patterns to be obtained. These patterns are very sensitive to crystallinity and are strong evidence of epitaxial growth.

Figures 12 and 13 are SEM cross sectional micrographs of epitaxial "pn" diode structures. The layer structure in Fig. 12 consists of a 0.3 micron thick boron doped layer with a 2.3 micron thick nitrogen doped layer grown on top. The boron doped layer is the black stripe. A polycrystalline boron doped layer grown during the same run produced a film 1.7 microns in thickness. Layer thickness control has been the major problem with our diamond epitaxy process. Figure 13 illustrates another problem that was encountered. The large rough boulder-like objects are polycrystalline inclusions into the epilayer film. This was a serious problem only near the edge of the substrate.

Grain Boundary Passivation

This concept of passivation is derived from a reported result that much of the non-diamond inclusions present in many CVD diamond films occur at the grain boundaries and that this intergranular material could be selectively etched away in an oxygen plasma. This approach now appears to be generally applicable to many phases of diamond processing including the fabrication

of single crystal devices. An example of some results from this technique is shown figs. 14a and 14b. Figure 14a depicts a boron doped polycrystalline layer, 0.6 microns in thickness, grown on top of an undoped layer. From this picture, the boron doped layer is only distinguishable by a slight change in grain size. Figure 14b is the same cross section after a low temperature oxidation. This oxidation (~450°C, 100% oxygen) creates strong SEM contrast differentiating the boron doped layer from the undoped layer. As SEM contrast is most affected by step height differences, the most straight forward interpretation of this effect is a doping dependent oxidation rate of diamond. In both these cross sectional pictures a conductive "potting" layer has been used to encapsulate the sample for SEM observation. This layer always appears as the topmost layer in the micrograph and is only there to facilitate SEM examination.

Figure 15 is a comparable SEM cross sectional micrograph to Fig. 14b except for an additional 2000Å thick nitrogen doped top diamond layer. The contrast of the nitrogen doped layer and the undoped layer are very similar, suggesting that the undoped layer contains sufficient nitrogen or nitrogen-like impurity to behave electrically and chemically similar to nitrogen doped diamond. This picture shows that the concept of defect etch and refill using nitrogen doped diamond is physically possible. Shown in this picture is an extremely smooth, "quasi-epitaxial", thin 2000Å thick nitrogen doped layer grown on a boron doped layer. This picture suggests that the process employed to grow this film grows in atomic layers without excessive (or any?) secondary nucleation. Another feature shown in this figure is the extremely conformal nature of the film as it covers a very rough faceted surface. In the proposed process, junction defects (grain boundaries) are to be etched and refilled with nitrogen doped diamond. Figure 15 suggests that the physical structure can be readily fabricated.

Diamond Diode Measurements

Nitrogen is a deep donor in diamond with an energy level ~1.5~-2.0eV below the conduction band. By imitating nature and doping the diamond films with nitrogen it is possible to compensate for the residual acceptor level and pin the Fermi level at 1.5eV below the diamond conduction band. Even though this is still far from the intrinsic resistivity of diamond, nitrogen doped diamond has a theoretical resistivity much higher than could be practically measured(>1 x 10^{16} Ω-cm).

In this application the junction properties of a pn diode using nitrogen "n type" doping are the main concern and not the resistivity of the nitrogen doped layer. In order to most easily verify junction operation, in contrast to Schottky behavior (metal/semiconductor junction), the first junctions investigated have been p^+/n^+ junctions. Figure 13 is a SEM cross section of one of these structures and Fig. 4 is a SIMS profile of the similar structure.

The purpose of the nitrogen doped region is to increase the built in voltage of a junction made to boron doped diamond so as to function as a gate diode. When working with heavily boron doped diamond the"n" layer serves an even more important function. All Schottky diodes contacts made directly to the boron doped layers are ohmic and not rectifying. Figure 16 is the current voltage characteristics of two separate Schottky barrier diodes. These diodes were both metallized with aluminum and differed only in the boron doping level, one was formed on 0.3 Ohm-cm material and the other on a 2.0 Ohm-cm film. The "n" is **required** to make a junction to these layers.

Figure 16 clearly shows only Ohmic behaviour at these doping levels. This dopant concentration already is lower than desired for optimum device behaviour but the results are consistent with other workers[6]. These diodes were made with the lowest doped material produced for this work.

Diodes were fabricated from wafers with the layer structure silicon/undoped diamond/boron doped diamond/nitrogen (oxygen) doped diamond. The diodes were fabricated by sputterir.g an array of aluminum dots on top of the nitrogen doped surface layer. Due to the surface layer, special provision has to be made to contact the P+ boron doped diamond layer. "Ohmic" contact to the P+diamond was made by subjecting some of the devices to a large current stress. This technique made the ohmic contact conduct excess leakage current for both polarities but produced substantially higher resistance than contacts deposited directly on the boron doped diamond layer. Figure 17 shows the schematic test set up.

Figure 18 plots representative current-voltage (IV) characteristics from diodes fabricated using a 500Å oxygen doped surface layer and Figs. 19 and 20 plots similar results from diodes that use a 500Å nitrogen doped surface layer. Most devices displayed asymmetric IV characteristics though none of the devices had a high rectification ratio indicative of a 1 volt (or greater) built in junction voltage. The diodes in Figs. 19 and 20 were fabricated from boron doped diamond layers having a nominal doping of $\sim 1 \times 10^{20} cm^{-3}$ boron, 0.05 Ohm-cm while the diode of fig.18 had a nominal doping of 0.1 Ohm-cm. Devices fabricated from structures

employing thicker "n-type" regions had higher resistance and lower rectification ratios. Devices using thinner "n-type" regions were ohmic. The diode in Fig. 20 was grown to have four times the nitrogen concentration of that in Fig. 19.

From the above SIMS analysis the "n-layer" doping densities were too low to achieve a high built-in voltage using a thin "n-type" layer. Due to the high resistivity of "n-type" regions doped with deep donors it is necessary for the layer to be thin enough so as not to dominate the IV characteristics. The low built in voltages are consistent with a Schottky barrier device formed with the aid of a thin low doped surface region.

This structure does allow diodes to be made on heavily doped active regions although it does not allow for the desired high built in voltages.

A nitrogen doping level of 4.5 x $10^{19}cm^{-3}$ was used in the diodes of Fig. 19 and an oxygen doping level of approximately 2.0 x $10^{18}cm^{-3}$ was used in the diode of Fig.18. An anomalous feature of the data is that the oxygen doped diode behaves electrically as if the doping density is higher than the devices doped with nitrogen. This latter behavior is also consistent with the oxygen doped diodes having higher series resistance. SIMS data is strictly chemical in nature and consequently not directly in conflict with this result. This difference can be due to differing electrical states of nitrogen. Nitrogen has two common energy states: substitutional (i.e.type Ib) with a donor energy of approximately 2 volts or clustered (precipitated platelets) with a donor energy of about 4.5 volts(i.e. type Ia). In this device approach only the substitutional donors will be completely ionized. The multienergetic nature of nitrogen may be responsible for the comparatively lower electrical activity when compared to the behavior of dissolved oxygen.

A comparison of both the rectification ratio and forward bias current of the nitrogen doped diodes show improved behavior at the higher nitrogen doping. The reverse saturation currents are the same while the diode in Fig. 20 with higher nitrogen has higher forward current. This suggests further improvement can come from optimization of the growth parameters to increase the incorporation of nitrogen.

Conclusions

Junction diamond pn diodes were made to heavily boron doped material demonstrating the concept of n type doping with deep donors. Schottky diodes were not able to be made to this material.

The major unresolved issue in diode construction is the incorporation of suitable high concentrations of n-type deep donor impurities. From the above data it is apparent here as in other works that boron dopes readily at any desired doping level. The device study has shown predictable trends in going from ohmic to rectifying behaviour with the insertion of an n-type junction layer and all indications are that if the doping density of the n-type layer could be increased the diode behaviour would improve. These results clearly support the original junction design. The original design concept did not make any allowances for grain boundaries and the current data suggest that to first order they are not of major concern.

The major area of improvement and focus is consequently on raising the doping level of deep donors.

References

1. M.W.Geis, D.D. Rathman, D.J. Ehrlich, R.A. Murphy, and W.T. Lindley, IEEE Dev. Let., **8** 341 (1987)
2. M.W. Geis, D. D. Rathman, J. J. Zayhowski, D. Smythe, D.K.Smith, G.A. Ditmer, in Diamond and Diamond-Like Materials Synthesis, G.H. Johnson, A.R. Badzian and M.W. Geis, eds. (Materials Research Society)
3. H. Shiomi, Y. Nishibayashi, and N. Fujimori, JAPS Conf. Abstract, Fall 1989
4. M.C. Hicks, C.R. Wronski, S.A. Grot, G.Sh. Gildenblat, A.R. Badzian, T.Badzian and R. Messier, J. Appl. Phys. **65** 2139 (1989)
5. N. Fujimori, T. Imai, and A. Doi, Vacuum **36** 99 (1986)
6. K. Okano, H. Naruki, Y. Akiba, T. Kurosu, M. Iida, Y. Hirose, and T. Nakamura, JJAP **28** 1066 (1989)
7. Y. M. LeGrice, R.J. Nemanich, J. Mort, D. Kuhman, M. Machonkin, F. Jansen, and K. Okumura, Appl. Phys. Lett. **55** 1121 (1989)
8. T. Kazahaya, S. Katsumata, and N. Hayashi, JAPS Conf. Abstract, Fall 1989

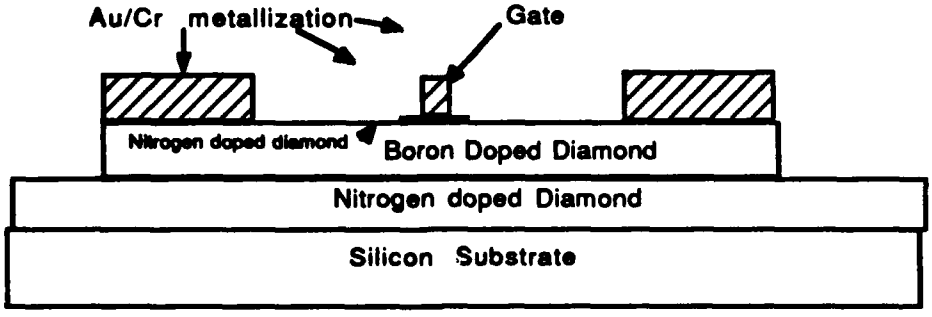

Figure 1. Schematic cross-section of the proposed Diamond Junction Field Effect Transistor(JFET). The device shown has been mesa etched for isolation. The combined height of the channel and the gate are only about 1000Å so that the isolation etch presents no topology problems. In a JFET all contacts are ohmic contacts which allow the use of only one metallization scheme which is Au/Cr in this figure for illustrative purposes but is not restricted to this metallurgy.

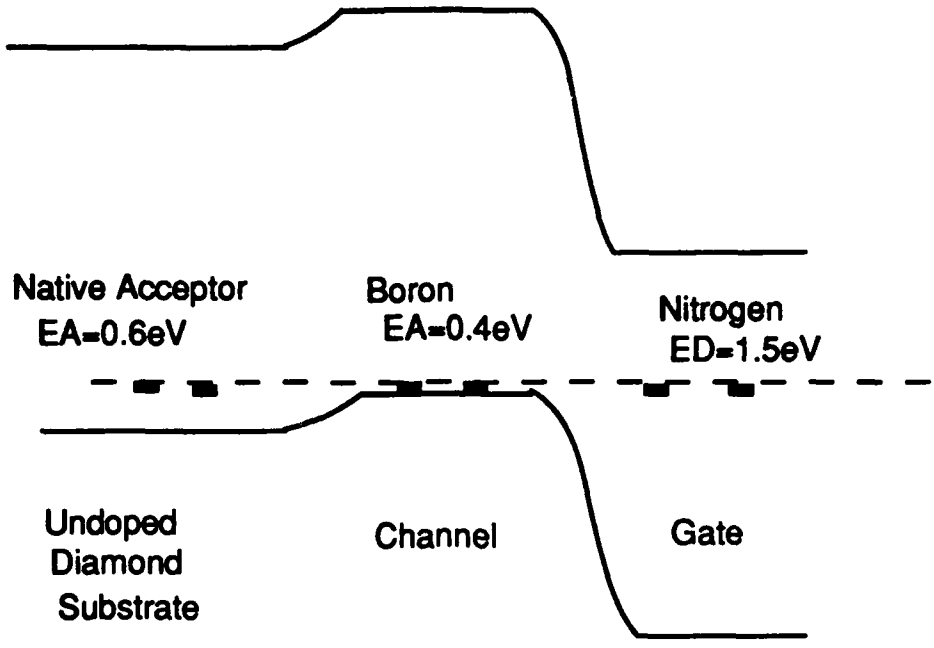

Figure 2 Hypothetical band diagram of a potential JFET configuration. In this figure the substrate Fermi level is controlled by a native acceptor defect level at 0.6eV above the valence band, the channel is doped with boron, a "shallow" acceptor and the gate is doped with nitrogen, a deep donor with an energy level 1.5eV below the conduction band. In an actual structure the native acceptors in the substrate would be compensated by nitrogen and have a resistivity and Fermi level as pictured in the above gate.

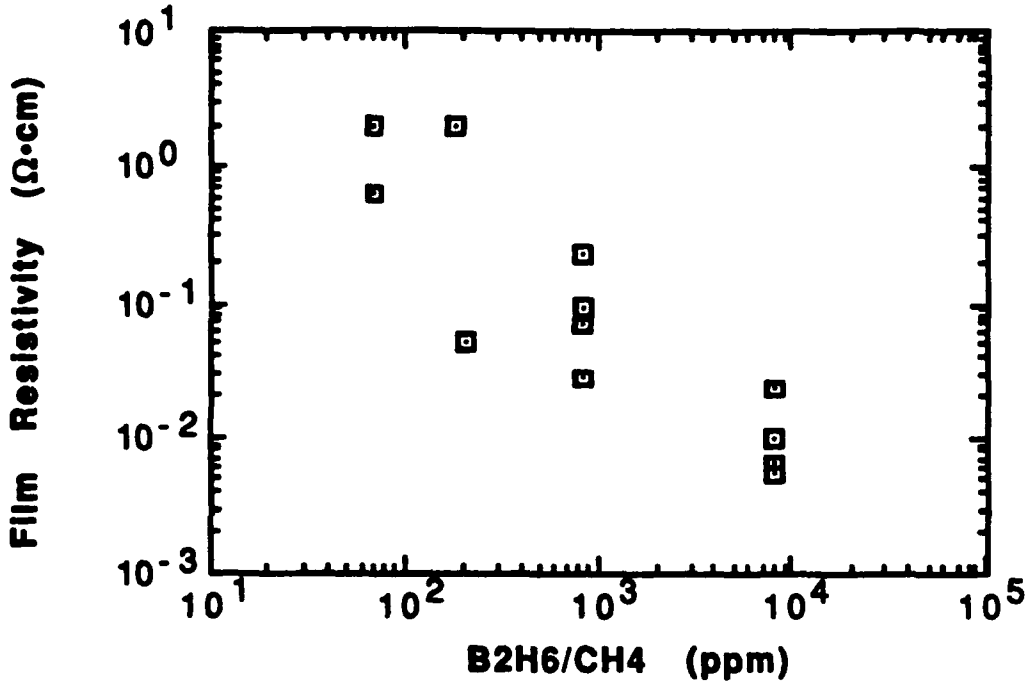

Figure 3. Diamond film resistivity versus the diborane to methane ratio present in the gas phase during layer growth.

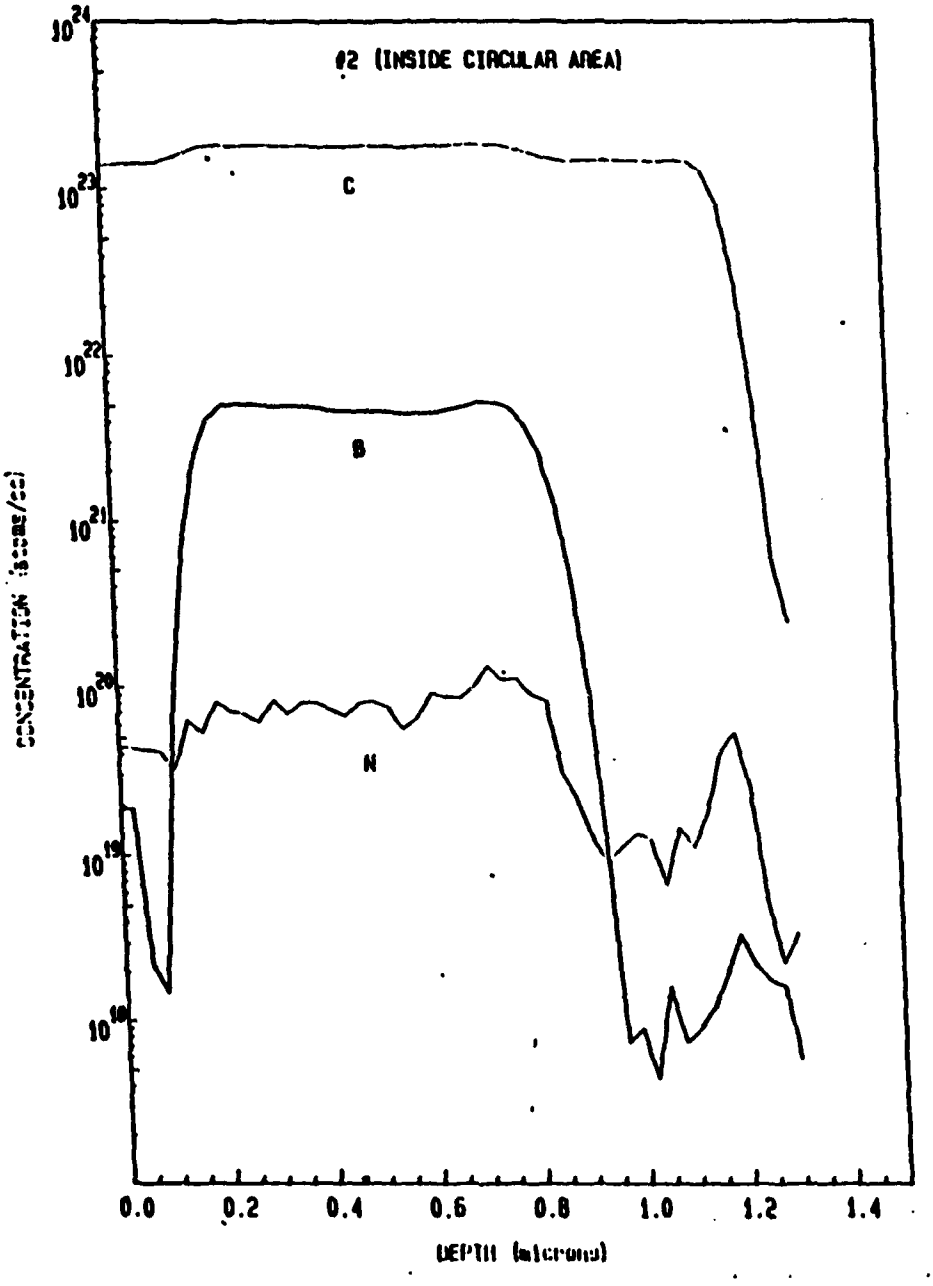

Figure 4: SIMS profile of the gate structure whose energy band structure is detailed in Fig. 2 The peak boron concentration has been recalibrated to $1.7 \times 10^{21} cm^{-3}$

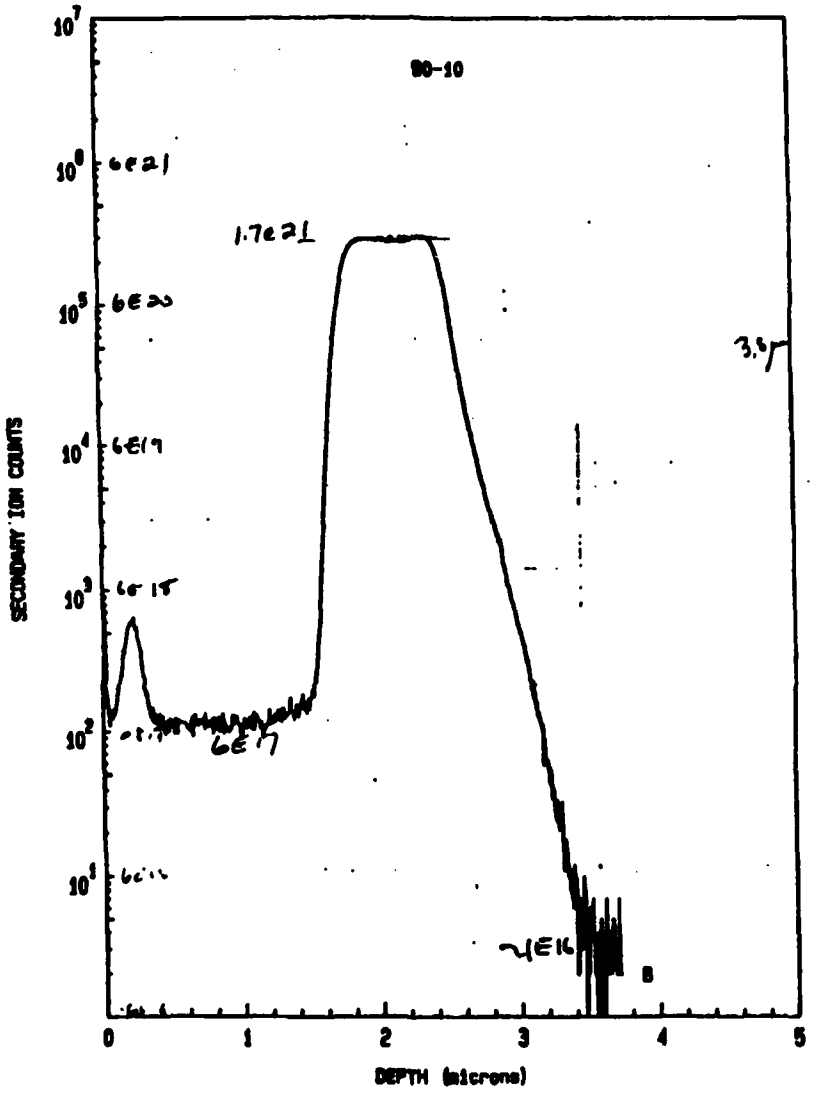

Figure 5: Boron SIMS profile of a structure similar to that of Fig.2. The undoped diamond surface region has been implanted with boron to improve the precision of the boron concentration measurement.

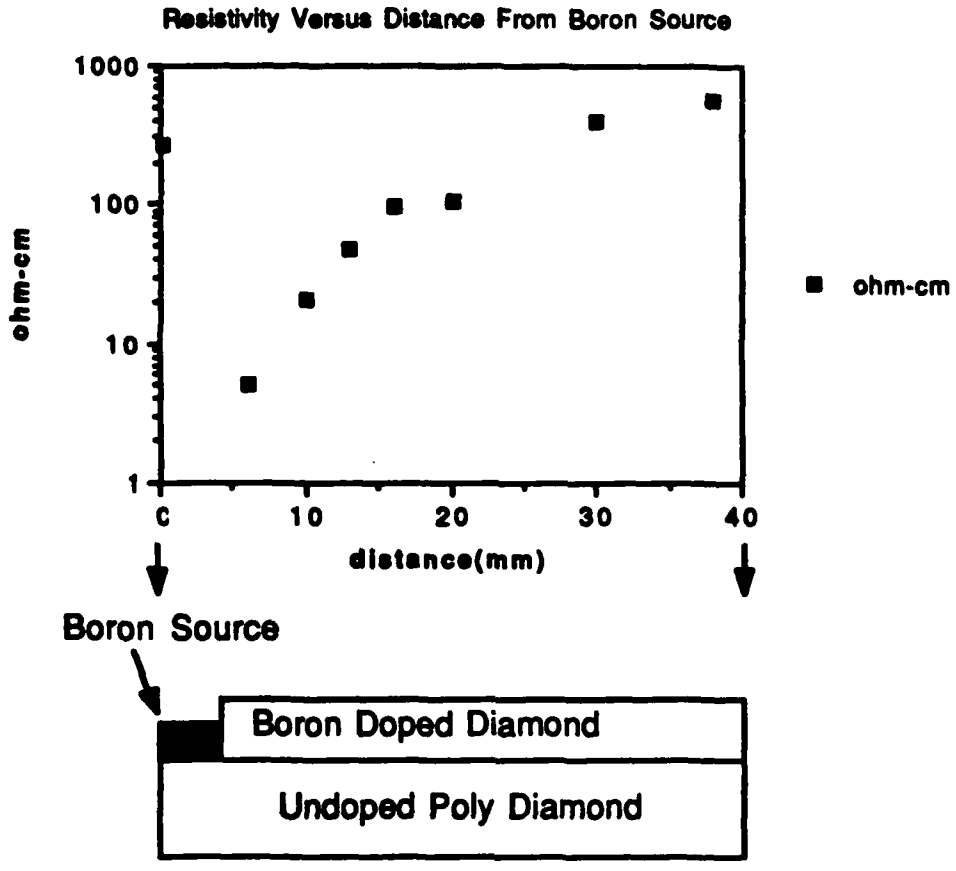

Figure 6: Plotted are the results of a diamond deposition incorporating in situ boron doping. The boron doping occurred by a gas phase reaction of the plasma with a solid boron source. The film thicknesses were 1500Å boron doped diamond on top of 3.0 microns of undoped diamond. The high resistance values are in error as the resistivity is calculated using 1500Å throughout.

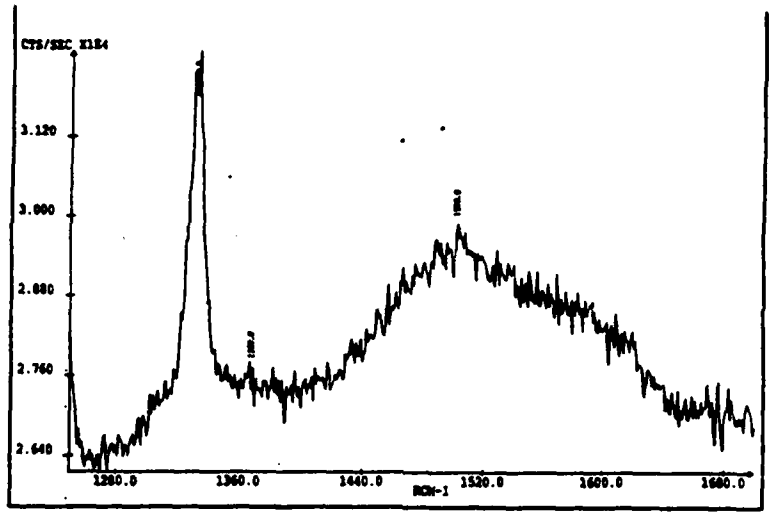

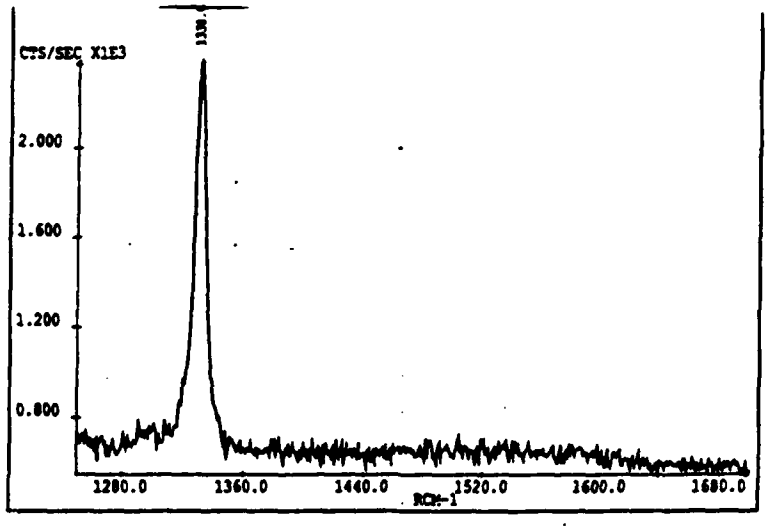

Figure 7: Raman spectra of a boron doped diamond film and an undoped film both grown in a DC plasma enhanced CVD reactor. The spectrum with the single sharp peak comes from a boron doped film

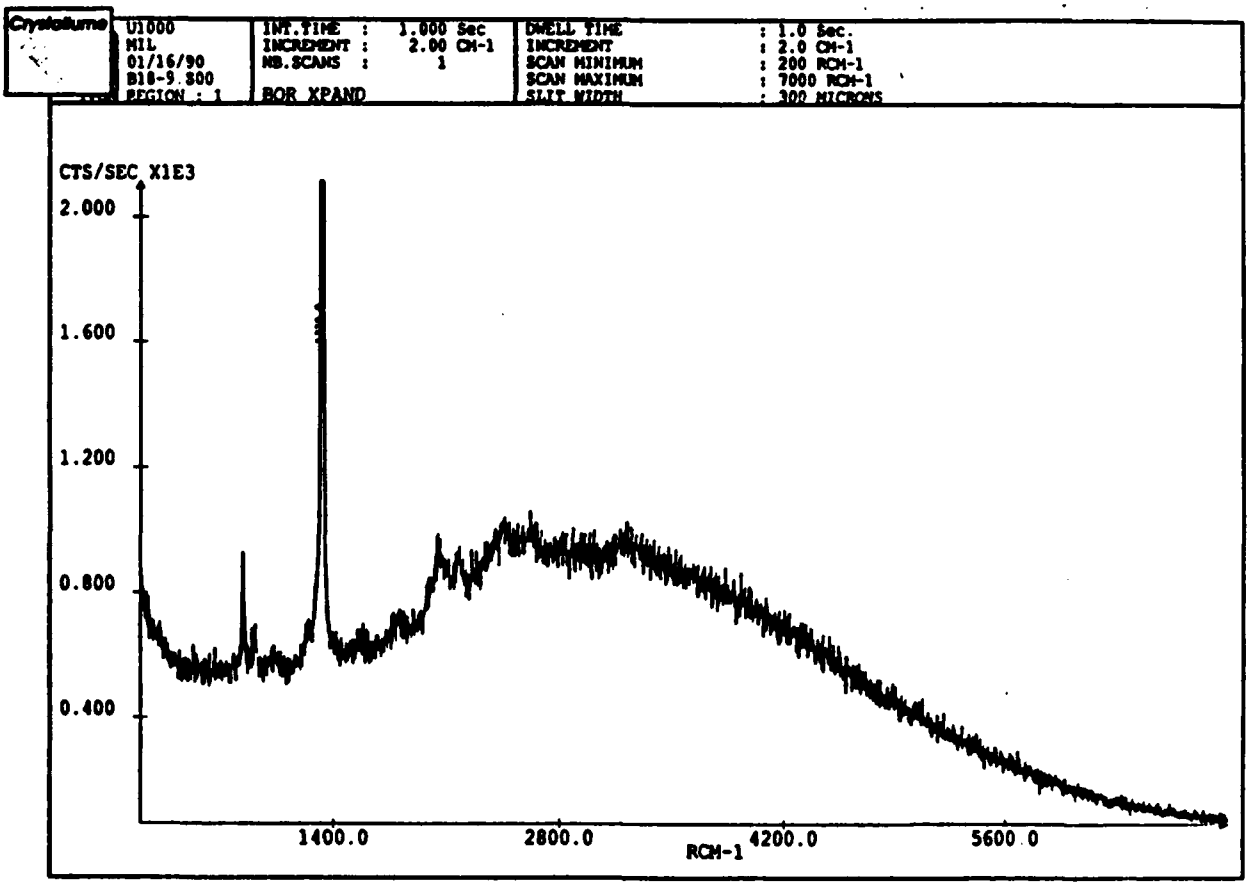

Figure 8: Raman spectra measured on a boron doped diamond layer grown on a (100) natural diamond substrate. The scale has been expanded, chopping off the top of the 1332 cm^{-1} diamond peak. The 1332 cm^{-1} peak intensity from the substrate is 1 x 10^5 cts/sec. The expansion is necessary to be able to detect the smaller Raman signal from the top layer in the presence of a strong signal from the substrate.

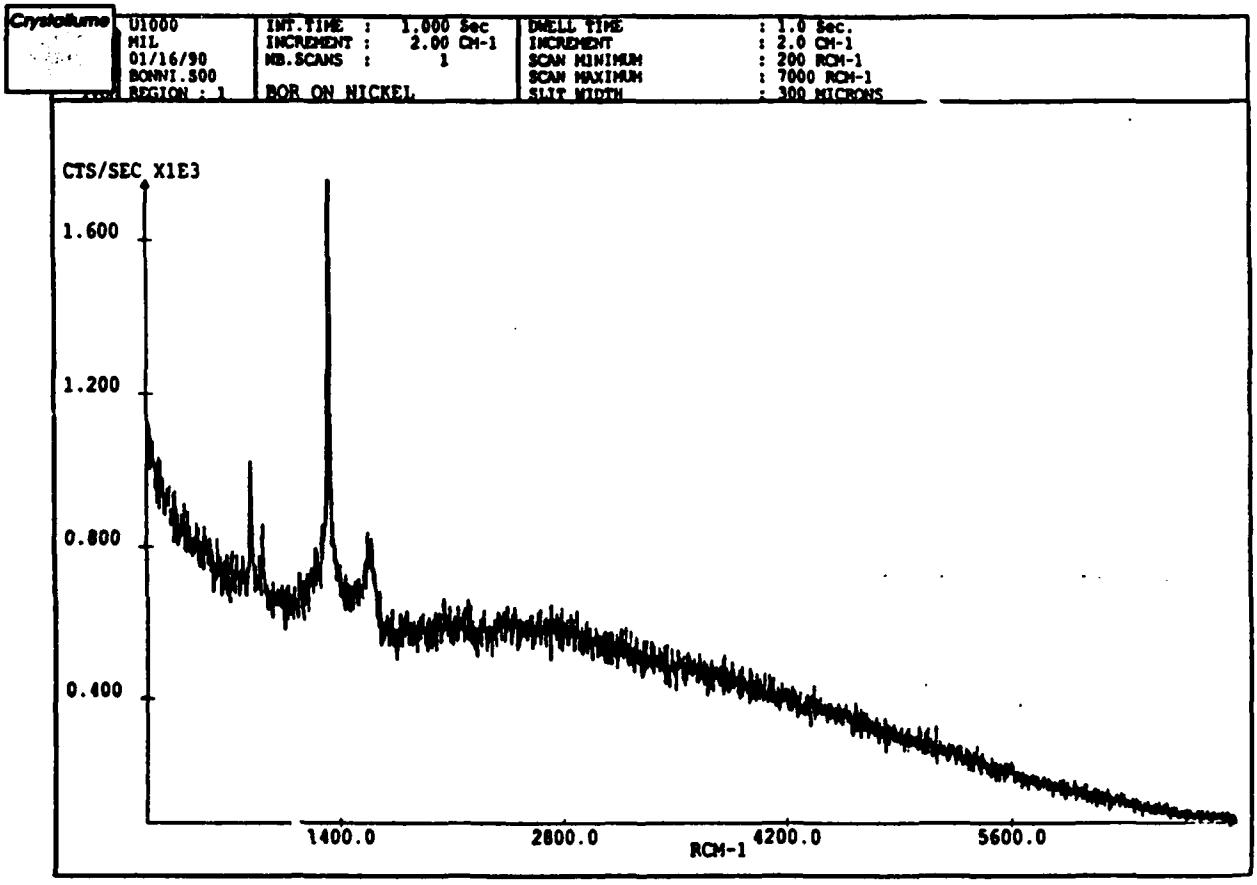

Figure 9: Raman spectra measured on a boron doped diamond layer grown on top of a nickel dot which had been sputtered onto a natural diamond substrate. As described in fig. 2 the scale has been expanded; the 1332 cm^{-1} peak intensity from the substrate is 1 x 10^5 cts/sec. As compared with fig. 2 this spectra shows a strong signal from non diamond bonded carbon as evidenced by the peak at 1550 cm^{-1}. The Raman contains signal from regions which are clearly polycrystalline as observed in the SEM.

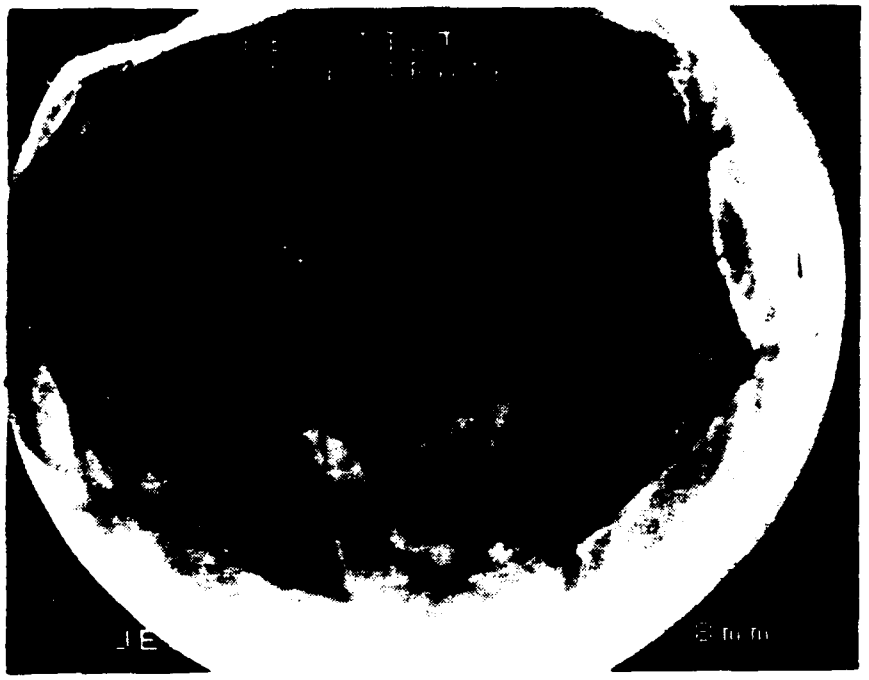

Figure 10: Backscattered electron channelling pattern recording measured on a cut and polished type IIA natural diamond. No specimen preparation or other alteration was performed on the natural gemstone. The sample's high resistivity interacts with this measurement and resulted in the spherical distortion of the pattern due to electron beam induced charging.

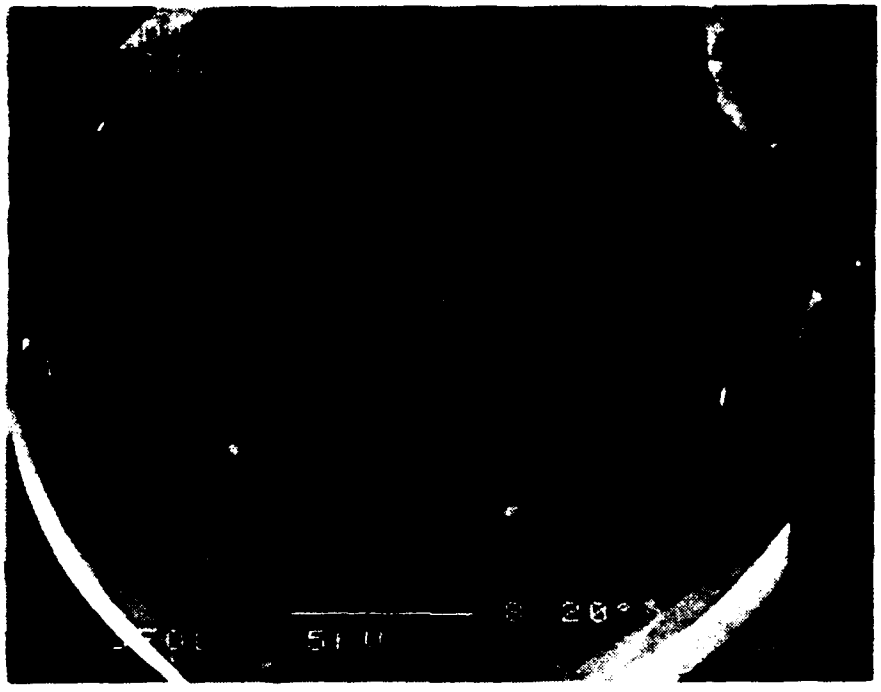

Figure 11: Backscattered electron channelling pattern recording measured on a epilayer grown on top of a cut and polished type IIA natural diamond. No specimen preparation or other alteration was performed on the natural gemstone. The sample's high resistivity interacts with this measurement and resulted in the spherical distortion of the pattern due to electron beam induced charging.

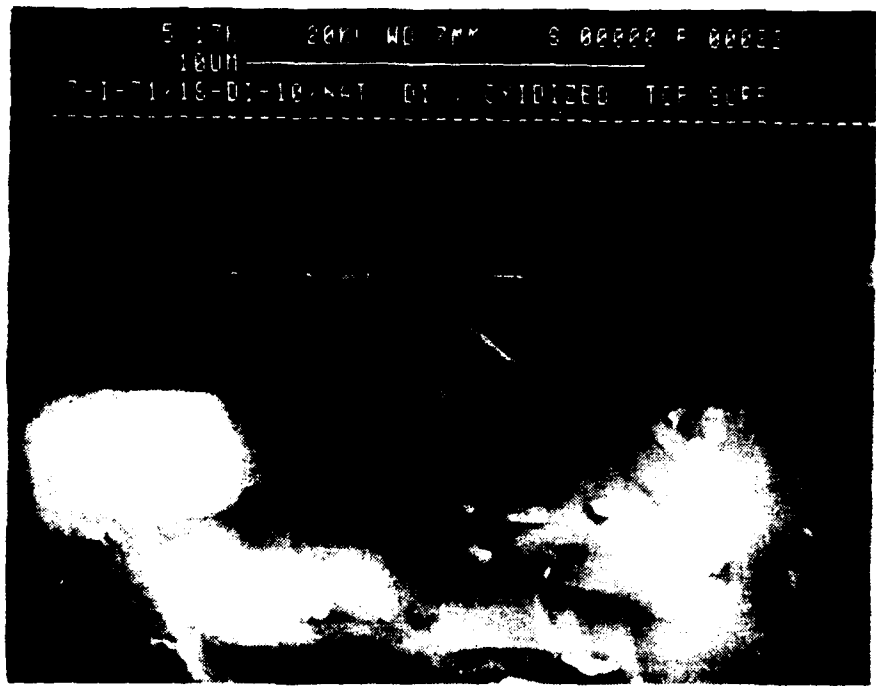

Figure 12: Cross sectional scanning electron micrograph of a two layer diamond film epitaxially grown on top of a naturally occurring type IIA diamond. The thin (0.3 micron) dark stripe is boron doped and the thicker (2.2 micron) top layer is nitrogen doped.

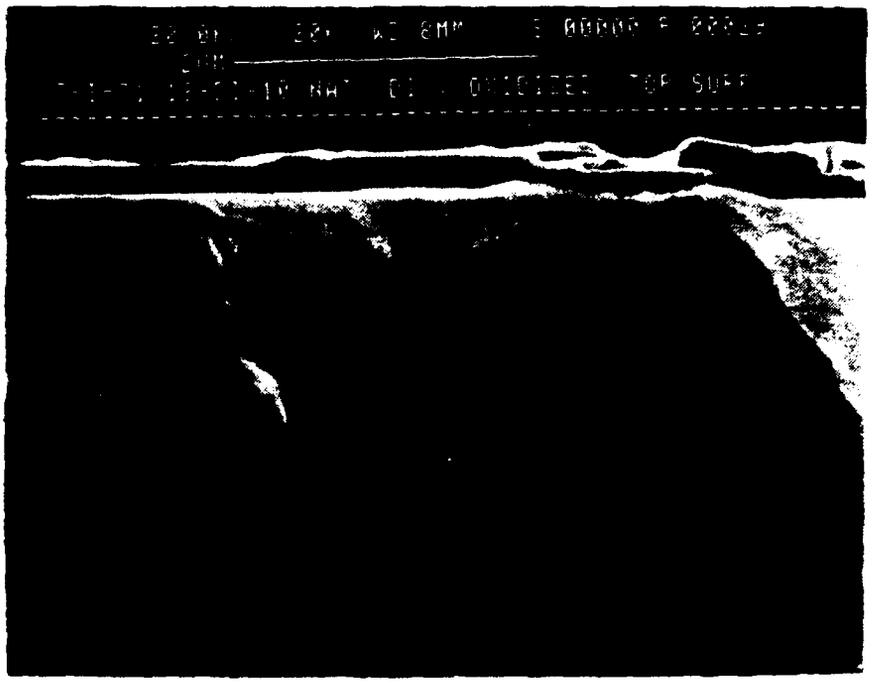

Figure 13: Cross sectional scanning electron micrograph of a two layer diamond film epitaxially grown on top of a naturally occurring type IIA diamond. The thin (0.3 micron) dark stripe is boron doped and the thicker (2.3 micron) top layer is nitrogen doped. This micrograph is taken from the edge region of the diamond wafer (1 x 1mm^2) and illustrates the polydiamond inclusions that occur in this region. The inclusions are the rock like structures in the top film above the born doped layer.

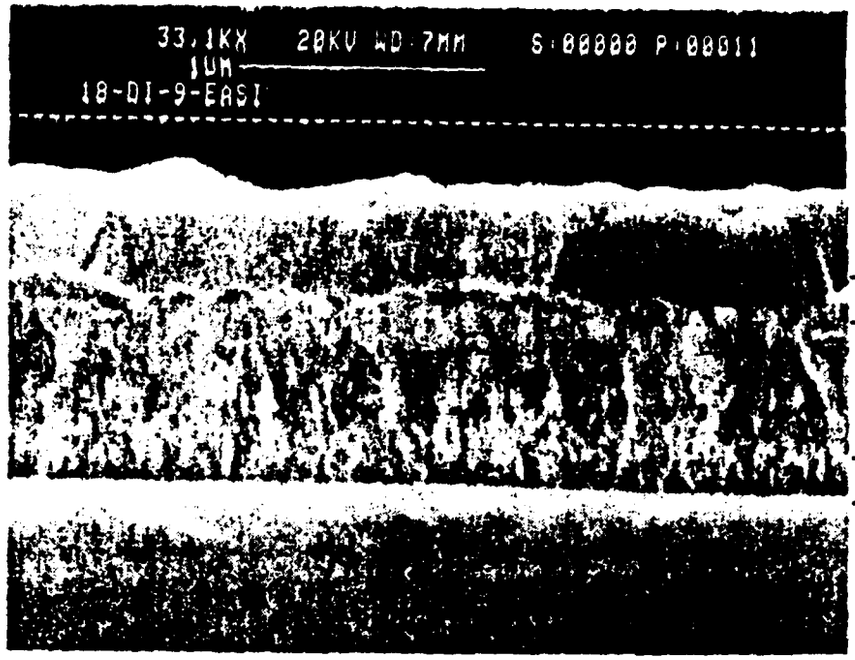

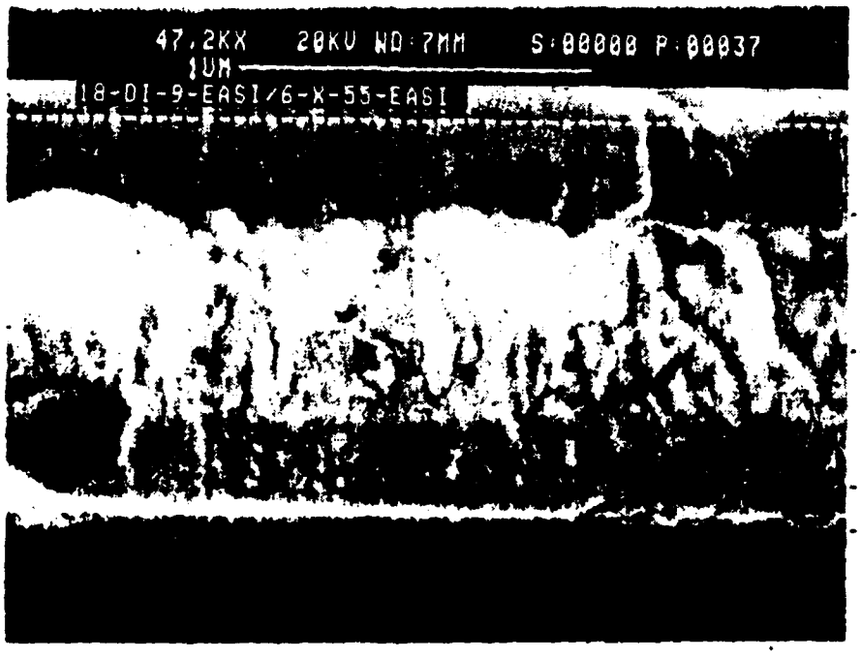

Figure 14A:. SEM cross sectional micrograph of a boron doped polycrystalline film. The initial substrate is a silicon wafer on which is first grown an undoped diamond film next followed by the boron doped layer. The topmost layer is a SEM potting layer used to improve the image quality. Figure 14B: SEM cross sectional micrograph of the identical piece pictured in fig.14A except for an additional low temperature oxidation.

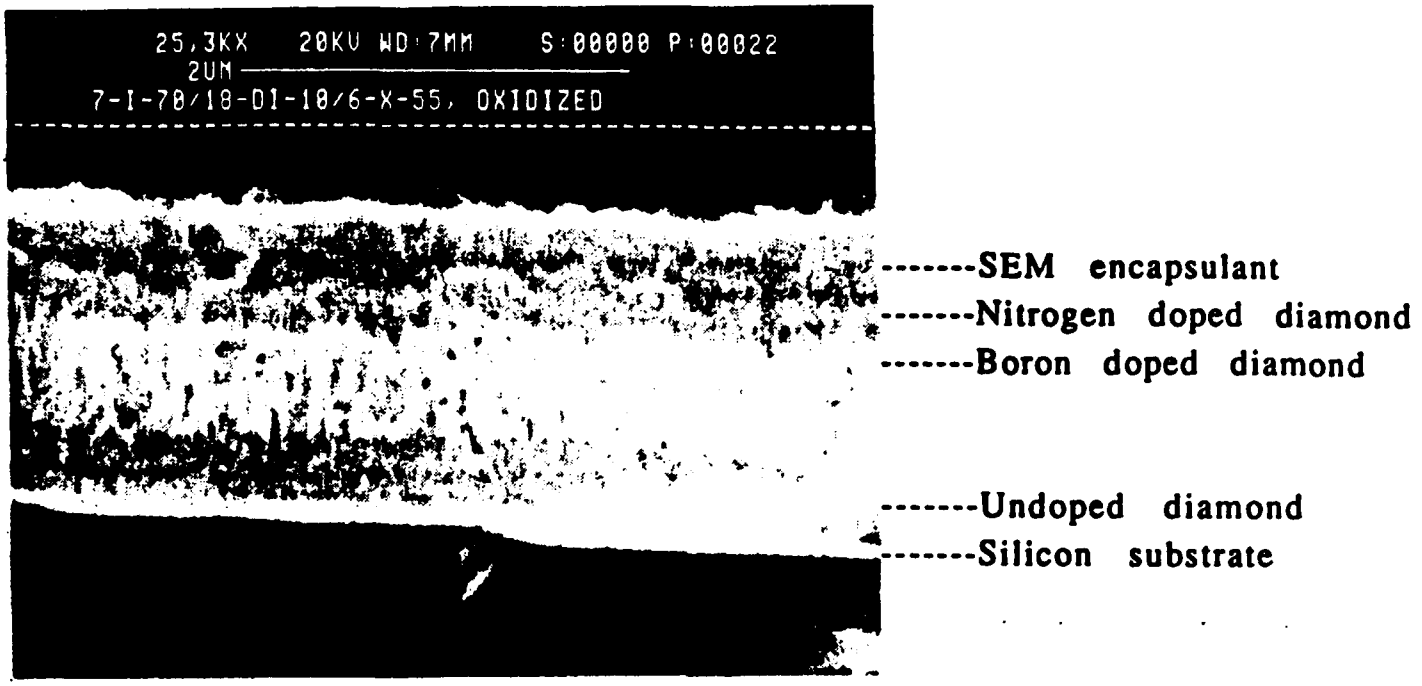

Figure 15: SEM cross sectional micrograph of a three layer polycrystalline diamond structure grown on a silicon wafer substrate. The layers are first undoped diamond, then boron doped diamond and finally a nitrogen doped diamond top layer. The sample has been subjected to a low temperature oxidation. The topmost layer in the micrograph is a SEM encapsulation used to improve image quality.

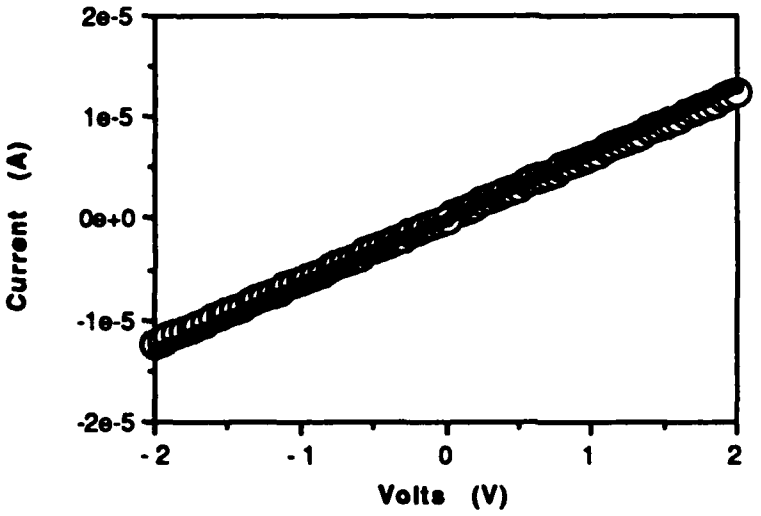

Figure 16: Current voltage characteristics measured on two diodes using aluminum metallization directly on diamond. The films resistivity was 0.6 Ohm-cm and 2.0 Ohm-cm boron doped polydiamond.

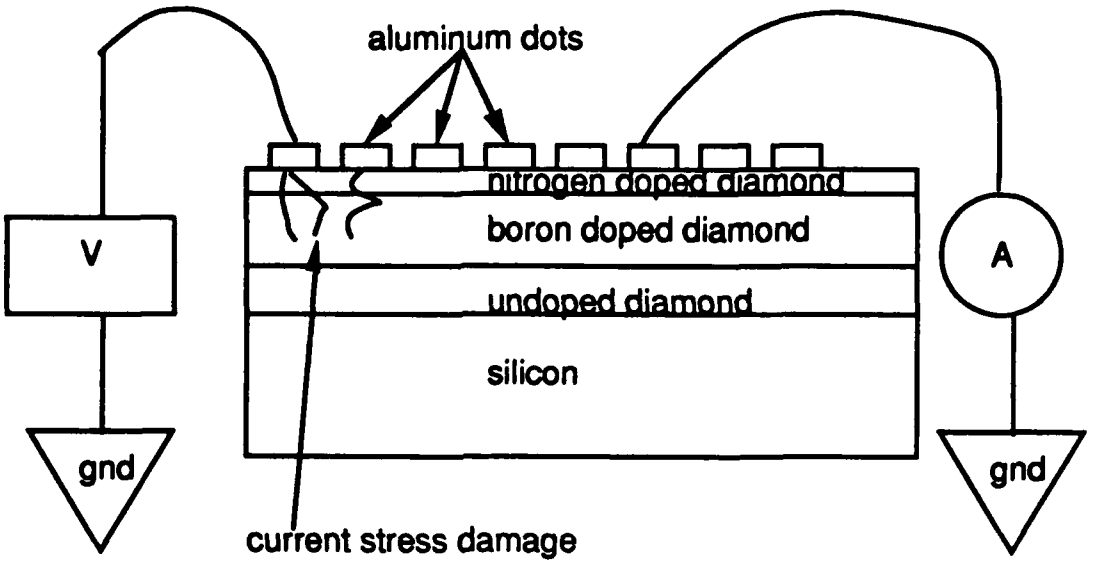

Figure 17. Diamond diode structure and schematic test set up.

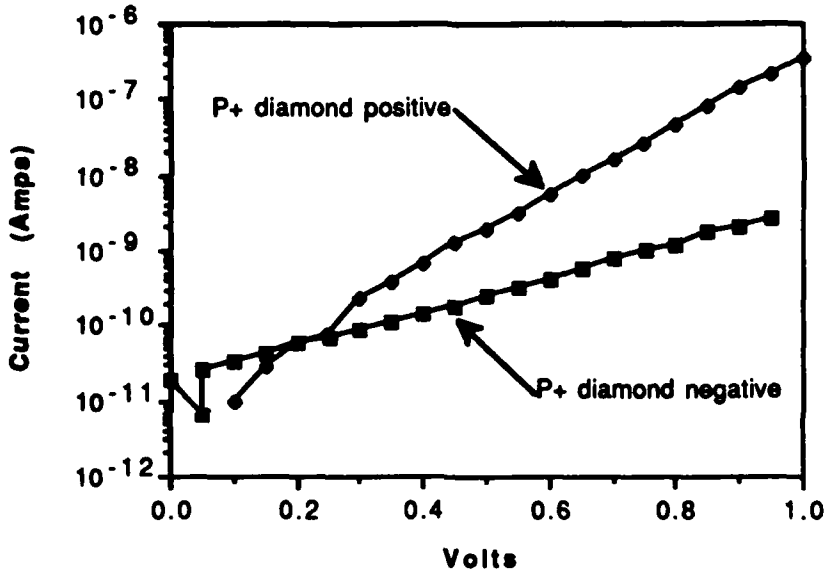

Figure 18. Current voltage characteristics measured on a diode using an oxygen doped n-type layer

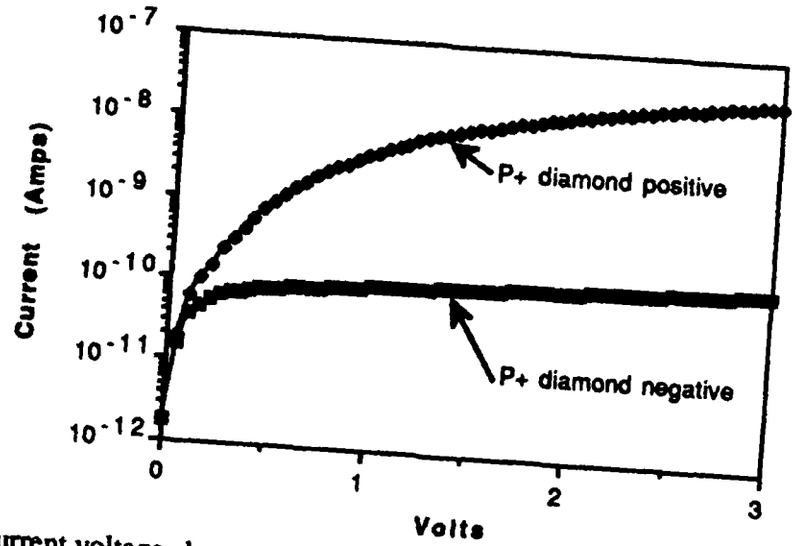

Figure 19: Current voltage characteristics measured on a diode using a nitrogen doped n-type layer.

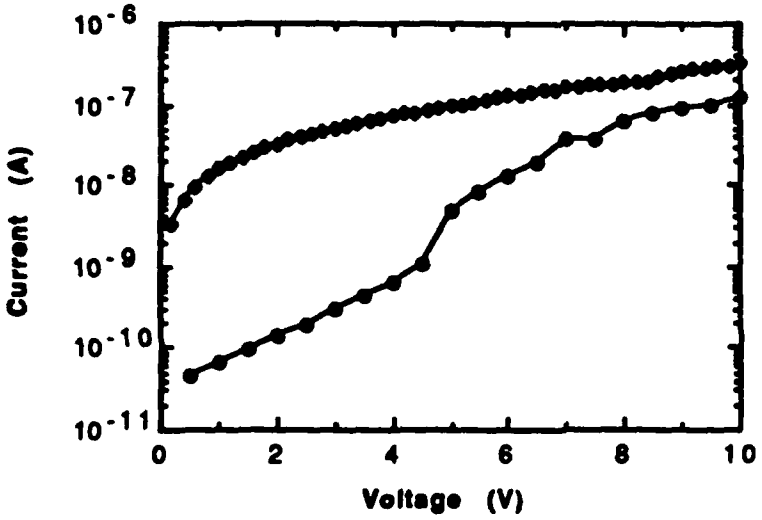

Figure 20: Current voltage characteristics measured on a diode using a nitrogen doped n-type layer.